Study of plasma dynamics in a modulated pulsed power magnetron discharge using a time-resolved Langmuir probe

L. Meng
Department of Nuclear, Plasma, and Radiological Engineering, Center for Plasma-Material Interactions, University of Illinois at Urbana-Champaign, Urbana, Illinois 61801

A. N. Cloud
Department of Materials Science and Engineering, University of Illinois at Urbana-Champaign, Urbana, Illinois 61801

S. Jung and D. N. Ruzic[a)]
Department of Nuclear, Plasma, and Radiological Engineering, Center for Plasma-Material Interactions, University of Illinois at Urbana-Champaign, Urbana, Illinois 61801

(Received 26 August 2010; accepted 28 November 2010; published 5 January 2011)

Modulated pulse power (MPP) technology is a derivative of high power pulsed magnetron sputtering that allows unprecedented user control over the growth process, although the critical time-dependent plasma properties during the power pulse have not been studied until now. Using a MPP plasma generator, pulses of custom voltage waveforms were generated and applied to the cathode of a 36 cm diameter circular planar magnetron. The *I-V* characteristics of the pulses are separable into distinct discharge stages. A time-resolved triple Langmuir probe was introduced to measure the temporal evolution of the plasma. Typical electron density of 5×10^{17} m^{-3} and electron temperature of 10 eV during the pulse were calculated from measured parameters. Plasma behaviors were observed to closely depend on the pulse waveforms. Various parameters, including pulse current, pulse frequency, pressure, and distance from the target, also affected the electron density and temperature, providing degrees of freedom to optimize the sputtering processes. The effects of each parameter on the pulsed plasma dynamics are discussed and then attributed to mechanisms of electron impact ionization, gas heating, and magnetic confinement. © *2011 American Vacuum Society.* [DOI: 10.1116/1.3528940]

I. INTRODUCTION

Pulsed magnetron sputtering has become an important industrial technique for the deposition of various thin films and coatings, demonstrating long-term process stability, reduced defect density, and improved film properties.[1–4] Different from these middle frequency pulsed dc magnetron sputtering, high power pulsed magnetron sputtering (HPPMS) has been developed as a new ionized physical vapor deposition technique featuring very high peak power density at the target (typically in the range of 500–3000 W/cm^{-2}) with low frequency (<10 kHz) and low duty factors (<10%) to avoid melting the target.[5,6] It generates a high-density plasma near the cathode and greatly enhances the ionization of sputtered materials.[7,8] These properties could benefit many physical vapor deposition (PVD) applications. A higher ion flux facilitates more conformal metallization of interconnect vias and trenches during integrated circuit fabrication.[9] The intense ion flux at the surface is expected to drastically modify the physicochemical and mechanical properties of the coatings.[10,11] In addition, particular effort has been invested in the tailoring of the optical properties of transparent metal oxides by HPPMS for a wide range of applications.[12,13]

Modulated pulse power (MPP) technology is a relatively new method of applying the basic principles of HPPMS. The MPP technique allows the generation of arbitrary voltage waveforms by modulating the durations and duty ratios of a batch of short "micropulses." More degrees of freedom are thus offered for additional process control during sputtering. MPP also enables a high power magnetron discharge with long pulse durations and a low probability of generating arcs.[14,15] It has been used to fabricate dense and uniform films with a higher deposition rate than the conventional middle frequency pulsed dc magnetron at a given average power, and a time-averaged plasma characterization of ion fluxes and their energy distributions was used to understand these merits.[16] However, few time-resolved plasma diagnostics during the MPP sputtering were done to further explore the mechanisms of this type of discharge. Temporal behaviors of plasma (e.g., electron temperature T_e and density n_e) during pulses are critical to study the plasma ignition and evolution in different discharge waveforms, and the interrelationships between plasma properties and various process parameters.

Typical time-resolved plasma diagnostic techniques used in HPPMS studies include optical emission spectroscopy,[5,17] double Langmuir probe,[18,19] and triple Langmuir probe (TLP).[20,21] The triple probe is a well-studied technique to measure the electron density and temperature that does not require sweeping the voltage of the probe tips. The theory is based on the assumptions of a Maxwellian electron energy distribution function (EEDF), collisionless thin sheath, and

[a)]Electronic mail: druzic@illinois.edu

no interaction between probe tips. The Maxwellian EEDF is a commonly used model of plasmas even though it is seldom exactly the case for low pressure magnetized plasmas. The latter two assumptions could be satisfied by appropriate selection of probe tip diameter and the distance between tips.[22] In the present study, a triple Langmuir probe was employed to investigate the dependence of electron temperature and density on the pulse shapes and other discharge parameters. A qualitative discussion of the features of the MPP discharge is presented based on the diagnostic results.

II. EXPERIMENT

The experiments were carried out in an MRC Galaxy sputtering tool featuring a 36 cm diameter circular planar magnetron. A water-cooled titanium target was used in all of the experiments presented. The distance between the substrate and target is adjustable, but typically fixed at 150 mm. A turbo pump is used to achieve a base pressure of 5×10^{-4} Pa. Argon gas was supplied to establish operational pressures ranging from 0.13 to 4.0 Pa by adjusting the gas flow rate. The pressure was monitored by a capacitance manometer.

Power was supplied to the magnetron by a Zpulser AXIA™ MPP plasma generator. More information on the circuitry, specifications, and operation of this MPP generator has been provided in Refs. 14 and 15. This plasma generator allows longer pulse durations (up to 3000 μs) than HPPMS does. Each of these long pulses (called as "macropulse") is composed of a sequence of micropulses (typically 20–30 μs in duration). By adjusting the "on" time (τ_{on}) and "off" time (τ_{off}) of the micropulses, macropulse width (500–3000 μs), and repetition frequency (10–400 Hz) using the Zpulser operating software, a macropulse of custom voltage and current waveform can be formed. Multistage pulses are usually formed and applied to the cathode. Low voltage and current are used for the initial step to initiate the plasma with reduced arcing effect, and then by increasing the pulse voltage and current, a high-ionization stage can be reached.[15] It should be clarified that the output voltage for each micropulse is not directly controllable, but varies with the τ_{on} and τ_{off}. The voltage will increase as τ_{on} increases and τ_{off} decreases.[14] The present MPP plasma generator can deliver a peak power up to 147 kW, a maximum average target power of 10 kW, and a maximum peak current of 247 A to achieve a strong ionization. The discharge voltage, current, and power were monitored by the Zpulser operating software. The effective sputtering area of the target is determined to be about 240 cm^2, so that the current density could always be calculated. For a typical peak current of 50–200 A, the peak current density ranges between 0.21 and 0.83 A/cm^2.

A TLP system was built as described in Refs. 21–23. Three tungsten wires (0.25 mm diameter) shielded by a multibore alumina tube serve as the probe tips. The three probes were parallel to the target surface and were normally located at 140 mm away from target, just above the substrate, as shown in Fig. 1. The exposed lengths of the probe tips are 8.8 mm and the separation of probes is 1.6 mm. Such dimensions are chosen to satisfy the collisionless thin sheath criterion and to prevent the interaction between probe tips. For a typical plasma condition (1 Pa, 10 eV, and 5×10^{17} m^{-3}), the sheath width (about 4 times Debye length) is estimated as 0.13 mm, smaller than the separation of tips, so that the interaction effects among the probes are negligible. The mean free path of electron-neutral collisions is calculated to be 8.10 mm, much larger than both the thickness of sheath width and the probe diameter to satisfy the collisionless thin sheath criterion. In order to use the probe in a strong metal deposition environment, each probe tip is kept centered in the bore without contacting the metal coated alumina tube. This is also important for keeping the stray capacitance between probe tips and ground as low as possible.[22] A schematic of the electrical circuitry of the probe data acquisition system is shown in Fig. 1. Probe 2 was allowed to remain at floating potential in the plasma, while probe 1 and probe 3 were connected through a battery pack so as to apply a bias V_{13} between them. The bias was set above 50 V to meet the requirement of the assumptions used to calculate the electron density and temperature which specify this bias be several times the electron temperature.[23] The current collected by probes 1 and 3 is obtained by measuring the voltage drop across a 10 kΩ resistor in series with the probe tips. This voltage drop (V_R) and the voltage difference between probe 1 and probe 2 (V_{12}) were measured using two differential probes (Tektronix P5200 with 50:1 attenuation).

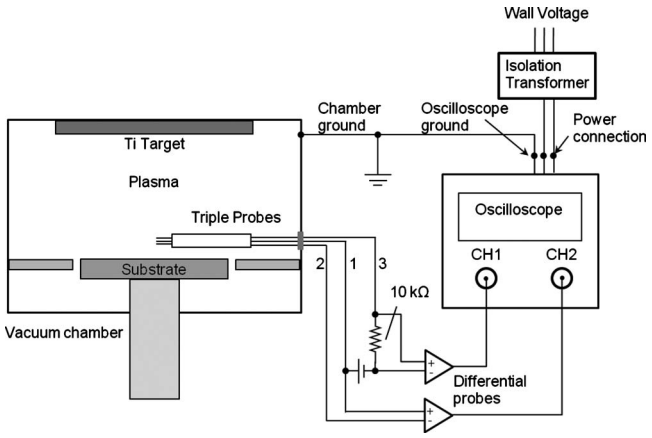

FIG. 1. Schematic diagram of the triple Langmuir probe system. The bias between probe 1 and probe 3 (V_{13}) is 58 V; probe 2 is allowed to float in the plasma discharge. The oscilloscope ground is isolated from the wall voltage and connected to chamber ground. Two differential probes are used to measure V_{12} and the potential drop V_R across a 10 kΩ resistor.

The signals were recorded using an Agilent Infiniium oscilloscope (1 GHz, 4 GSa/s). The oscilloscope ground was isolated from the wall outlet by an isolation transformer and then connected to the chamber ground, which greatly reduced the 60 Hz noise from the wall voltage.

After the acquisition of the V_{12} and V_R (so that current I_{13} between probe 1 and 3 could be obtained), the electron temperature T_e and electron density n_e were calculated using Eqs. (1) and (2),[22,23]

$$[1-e^{-(eV_{12}/kT_e)}]/[1-e^{-(eV_{13}/kT_e)}]=1/2, \quad (1)$$

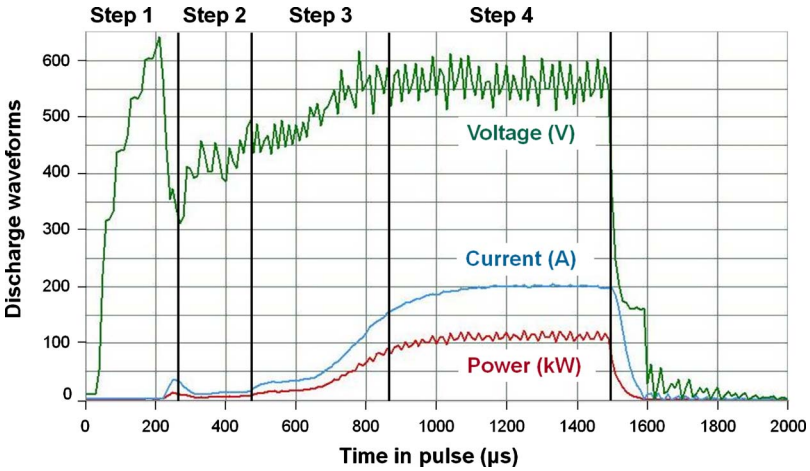

FIG. 2. (Color online) Typical waveforms of the discharge voltage (V), current (A), and power (kW) during MPP sputtering of titanium with argon. Four distinct discharge stages are observed.

$$I_{13} = \exp\left(-\frac{1}{2}\right) A_p e n_e \sqrt{\frac{kT_e}{M}}, \tag{2}$$

where A_p is the surface area of the probe tip, k is the Boltzmann's constant, and M is the mass of ions. In this article, argon mass is used. This will cause a certain error in the calculated electron density n_e since metal ions also exist and their density can be comparable with that of argon ions in a MPP discharge.[15] Fortunately, this error is always below 10% even if only titanium ions exist in the plasma. This is acceptable considering the uncertainties of the measured T_e and n_e caused by data acquisition are estimated to be 15%–20%. It should also be stated that the triple probe method introduces some intrinsic error due to using three points instead of the whole Langmuir probe I-V curve. Such error analysis has been described in Ref. 22. Meanwhile, the time resolution of the measurement is on the order of the intrinsic response time of the probe itself (≤ 1 μs).

Using this triple Langmuir probe system, the time-resolved plasma parameters were measured throughout the MPP pulses to examine the different discharge stages in the pulses. The effect of different parameters such as the pulse shape, discharge current, pulse repetition frequency, gas pressure, and the distance to the target were investigated.

III. RESULTS AND DISCUSSION

A. *I-V* characteristics of MPP discharge

The *I-V* discharge characteristics of the MPP generator were studied prior to the triple probe measurements. The voltage applied to the cathode and discharge current were both recorded. A typical set of discharge waveforms are shown in Fig. 2. The macropulse had been programed to be 1500 μs long, consisting of micropulses of 6 μs on and 34 μs off in the initial 500 μs and those of 12 μs on and 20 μs off thereafter. Four different steps can be defined from the waveforms. The first one could be identified as the "ignition" stage. A steep voltage spike was observed which is common at the pulse transients to promote the establishment of plasma.[20,24] The step ends with a small surge of current, implying plasma has been generated and a discharge is maintained. Subsequently, the discharge enters step 2 and becomes similar to a normal dc discharge. The discharge voltage and current are relatively low (450 V and 10 A, respectively). The peak power is less than 5 kW. As the higher duty-ratio micropulses are applied after 500 μs, both current and voltage start to rise. During the off time of the pulse, electrons diffuse to the target and chamber walls so the electron density decays with time. The higher duty-ratio pulses feature shorter off time for the electron loss to occur, resulting in the building of higher electron density. At some critical point, the electron density in the sheath/presheath region becomes high enough to effectively ionize the atoms, including the sputtered titanium atoms which has even lower ionization potential of titanium (6.8 eV) than that of argon (15.8 eV).[25] These ions are then collected by the cathode to generate a faster rise in current. In the final step, a new "steady state" is reached and maintained as a high power self-sputtering discharge. The discharge voltage is ~550 V, current is ~200 A, and the peak power is ~110 kW. It should be noted that even though this "high power discharge" stage is desired, the weak pulses regime is necessary to ensure the discharge can be initiated without an overvoltage, as well as to suppress arc formation during the high power mode of operation.[15] The modulation of the pulse voltage and current is one important advantage of the MPP technology.

B. Triple Langmuir probe measurements

1. Test of the triple Langmuir probe

Using the triple probe system described above, time-resolved plasma diagnostic studies were carried out in MPP discharge plasmas. Different pulse recipes have been programed and used for the Langmuir probe measurements. Table I summarizes the pulsing parameters and test conditions for each of them and more details of the pulse recipes are described in the corresponding experiment results section.

The argon gas pressure was 0.67 Pa and the probe was placed at the radial center of the chamber 140 mm from the target. Pulse recipe No. 1 was programed to start with some

TABLE I. Different pulse recipes used for the triple Langmuir probe measurements.

Recipe No.	Pulsing file[a] (μs)	Pulse length (μs)	Repetition frequency (Hz)	Gas pressure (Pa)	Average power (kW)	Probe distance to target (mm)
1	Alternate $\tau_{on}/\tau_{off}=16/8$ and $\tau_{on}/\tau_{off}=10/25$	600	60	0.67	1.5	140
2	$\tau_{on}/\tau_{off}=10/26$	1450	100	0.67	1.5	140
3	$\tau_{on}/\tau_{off}=10/12$	630	100	0.67	1.2	140
4	$\tau_{on}/\tau_{off}=10.5/15$	3000	93	0.13–4.0	3.3–6.2	60–140
5	$\tau_{on}/\tau_{off}=8/24$	1500	55–190	0.67	0.6–2.2	140

[a]The listed pulse files are simplified to represent the actual pulse files.

weak micropulses (8 μs on and 25 μs off) and after 250 μs, it continues with an alternate of "strong" (16 μs on and 8 μs off) and "weak" pulses (10 μs on and 25 μs off). The corresponding discharge waveforms are shown in Fig. 3(a), exhibiting the familiar multiple stages of the MPP pulse. Some spikes of current and voltage have been generated intentionally which demonstrates the capability of MPP to produce arbitrary discharge waveforms. A close look shows that when the current rises, the voltage tends to fall and vice versa. This is likely because the MPP plasma generator is powered by a dc plasma generator that does not respond instantaneously and tries to maintain a constant power output.

The triple probe results are shown in Fig. 3(b). Both n_e and T_e oscillate significantly; the timing of the spikes matches well with the discharge waveforms. This not only proves the functionality of the time-resolved triple probe, but also shows the viability of controlling the plasma parameters by tuning the pulse shapes in MPP. Also observed in Fig. 3(b) is that T_e has an opposite behavior of oscillation as n_e. Basically, the density n_e has the same trend as current. A higher n_e produces more ions and thus enhances the cathode current proportionally. The electron temperature T_e has a similar trend as the voltage. As the cathode voltage drops, ion-induced secondary electrons are not accelerated into the plasma as forcefully and therefore, the electron temperature drops. This drop could be very fast considering the quick response of electrons to the voltage change. Another possible reason for the opposite trends of T_e and n_e is that as current (or n_e) increases, more sputtered material will immediately cool the plasma through collisions with electrons, so T_e drops correspondingly. As for the average trend through the whole pulse, n_e increases from approximately 3×10^{17} to 6×10^{17} m^{-3}, while T_e gradually decreases from about 20 to 4 eV. It should be kept in mind that at the beginning of the pulse, the plasma is highly non-Maxwellian, so that the average electron energy is a more appropriate term to use rather than the electron temperature T_e. After the current ramps up, a higher density plasma is created, implying a much more violent and rapid return of ionized metal ions to the target. This enhanced ionization comes at the expense of electron energy. Due to collisions in the sheath/presheath region, the electrons will not be accelerated by the full sheath potential and therefore not be as energetic.

2. Effect of the discharge current

The effects of various discharge conditions on the plasma were studied. Two different pulses recipes, No. 2 and No. 3, were used to create different steady state pulse currents, 40 and 75 A, by varying the on and off time of the micropulses. The same pressure of 0.67 Pa was used and the probe was located at the center of the chamber 140 mm from the target. As shown in Fig. 4, raising the pulse current led to an increase of n_e from about 2.5×10^{17} to 5×10^{17} m^{-3}, however,

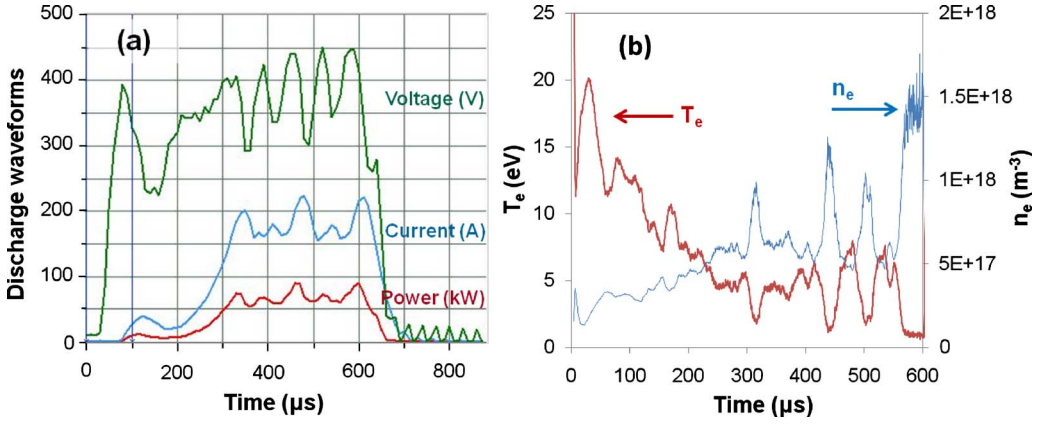

FIG. 3. (Color online) (a) Discharge voltage, current, and power waveforms from pulsed sputtering of titanium in 0.67 Pa of argon. (b) The corresponding n_e and T_e during the pulse. Probe was located under the center of the cathode at a range of 140 mm.

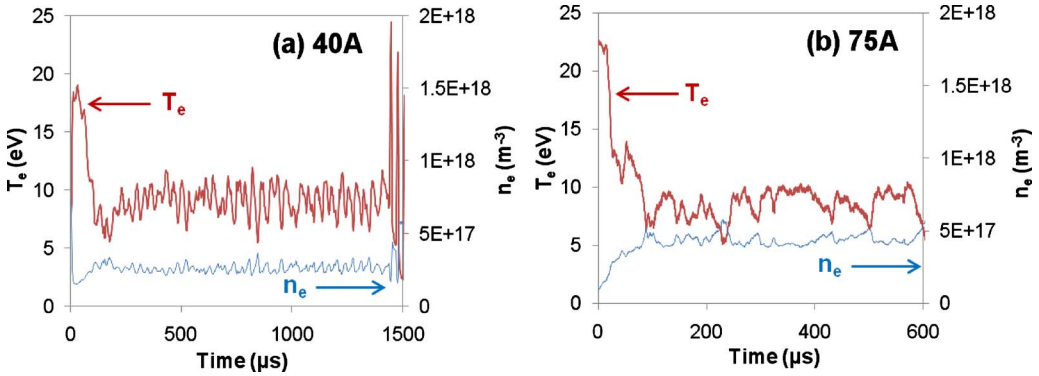

FIG. 4. (Color online) Evolution of n_e and T_e for two pulse recipes with different pulse currents, (a) 40 A and (b) 75 A. Titanium target, 0.67 Pa of argon. Probe was at the center of chamber and 140 mm from the target.

the electron temperature during the steady stage did not change significantly at about 9 eV with a possible slight decrease. An increase of the average discharge current to 175 A (by recipe No. 1 as used to obtain Fig. 3) increased n_e to about 6×10^{17} m^{-3}, whereas reduced T_e to 4 eV. Again, this trend is likely caused by the electrons losing energy by ionizing metal atoms in the sheath and presheath region where an electric field is present.

By varying the pulse recipes, higher discharge current could be achieved, increasing the electron density. However, the density is not directly proportional to the current, which is probably because the measurements were performed on the substrate level and there was considerable electron loss to the chamber walls before reaching the probes.

3. Effect of pressure

The pulse recipe No. 4 was tested with varied chamber pressure from 1.3×10^{-1} to 4.0 Pa. The probe was in the same position (140 mm from target). The triple probes showed similar T_e and n_e curves for the two cases, for example, an obvious step at 2000 μs originated from the pulse programming. At higher pressure, n_e rises slightly, e.g., from 3×10^{17} to 4×10^{17} m^{-3} at about 1500 μs (Fig. 5). Meanwhile, T_e was observed to significantly decrease from 11 to 6 eV. The density goes up with pressure since there is more gas to ionize, i.e., the frequency of electron impact ionization increases. It should be noted that the discharge voltage was observed to decrease as the pressure increased, approximately from 340 to 270 V. Obviously, the discharge at higher pressure requires much lower cathode voltage to maintain equilibrium. The sheath potential was thus lowered and consequently electrons gain less energy from the sheath acceleration. Another reason for lower T_e is that the electrons will undergo more collisions in higher pressure condition and drop more energy toward thermalization. Since pressure is one of the most common parameters in PVD processing, the effects of pressure on the pulsed plasmas can be utilized for optimizing the processes based on individual requirements for the electron density and temperature.

4. Effect of repetition frequency

The above experiments have shown that the τ_{on} and τ_{off} of the micropulses or duty ratios play an important role in the discharge characteristics and the plasma parameters. In HPPMS studies, much attention has been paid to the pulse on and off time, which are deemed as the main contributing factors to the observed plasma dynamics.[8,26,27] In a MPP discharge, not only can the micropulses be switched to on and off with programed lengths, but the macropulses can also be controlled in a similar way. Recipe No. 5 uses a macro-

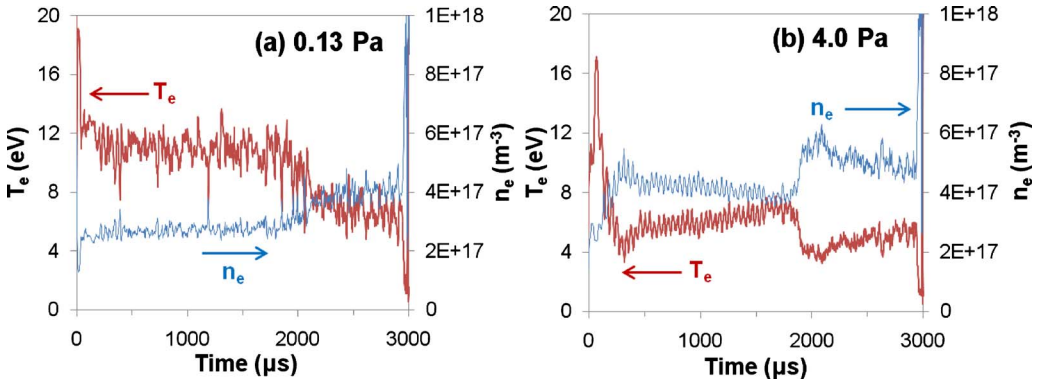

FIG. 5. (Color online) n_e and T_e during pulses under different pressures, (a) 0.13 Pa and (b) 4.0 Pa. The same pulse recipe was used to sputter titanium and the probe was at the center of chamber and 140 mm from target.

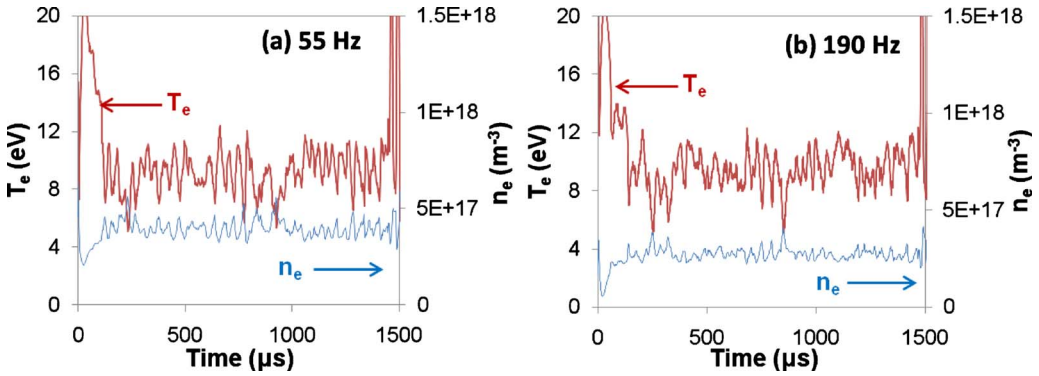

FIG. 6. (Color online) Time resolved n_e and T_e with different macropulse repetition frequencies, (a) 55 Hz and (b) 190 Hz. The pulse shape was the same, titanium target, 0.67 Pa of argon, and the probe was at the center of chamber and 140 mm from target.

pulse of 1500 μs duration, and the off-time between pulses can be set to control repetition rate as desired. The triple probe shows that the electron density is lower at a repetition rate of 190 Hz (2.5×10^{17} m^{-3}) compared to 4×10^{17} m^{-3} at 55 Hz while T_e barely changes (Fig. 6). It should be noted that the average power was higher at 190 Hz (2.2 kW compared to 0.6 kW at 55 Hz) to heat up the background gas and sputtered materials to a higher temperature. According to Juliano *et al.*,[28] a higher gas temperature will lead to a higher diffusion constant and a shorter residence time of atoms. As a result, the ionization fraction and thus electron density were lowered as observed. It has also been suspected that a "rarefaction" effect[27,29] happens at higher repetition frequency with more atoms being sputtered in a given time which might enhance the depletion of gas atoms around target through collisions and as a result, the electron density decreases similarly to the manner observed in the lower pressure condition. Studies will be performed to verify or exclude this effect.

5. Effect of distance from target

Using recipe No. 4, the probe was moved from 140 mm away to 60 mm away from the target to measure the plasma. The same pulse recipe as used for the pressure tests was used here at a pressure of 0.67 Pa. Figure 7 shows the temporal evolution of n_e and T_e at two locations, respectively. As the probe gets closer to the target, n_e increases from 5×10^{17} to nearly 8×10^{17} m^{-3}, while T_e decreases significantly from 11 to 4 eV. It is easy to understand the higher electron density near the target considering the strong magnetic confinement of electrons and thus intense ionization reactions there. As the plasma diffuses out toward the chamber wall and substrate, the density naturally decreases. The electrons are confined by the magnetic fields near the target, allowing only the higher energy electrons to escape and causing the average electron energy to be higher further from the target. Pressure balance is also in play. If the density decreases, the temperature should rise accordingly.

IV. CONCLUSIONS

A Zpulser plasma generator was applied to a planar magnetron to study MPP sputtering. By changing the arrangement of micropulses in a macropulse, arbitrary pulse shapes were achieved. The *I-V* characteristics showed that a MPP macropulse is composed of multiple stages. A time-resolved triple Langmuir probe system was employed to investigate the temporal evolutions of n_e and T_e under various discharge parameters. A typical n_e of 5×10^{17} m^{-3} and T_e of 10 eV

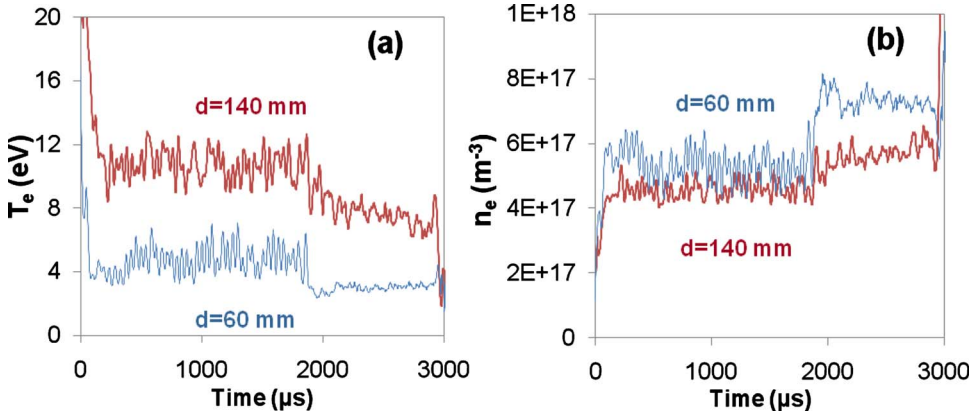

FIG. 7. (Color online) Temporal evolution of n_e (left) and T_e (right) in the pulse measured at different locations, 140 mm from target (close to substrate level) and 60 mm from target. The same recipe was used as in Fig. 5 to sputter the titanium target in 0.67 Pa argon gas.

were obtained on the substrate level. By varying the micropulse parameters, higher discharge current could be achieved along with higher electron density; however, the very collisions of electrons with metal atoms responsible for the rise in density result in a lower electron temperature. Higher repetition frequency of macropulses leads to a higher gas temperature, which reduces the ionization and thus electron density. Higher pressure during the MPP discharge enhances the electron collisions with the background gas atoms, and as a result, higher n_e and lower T_e were measured. Moving the probe closer to the target revealed increased electron density but reduced electron temperature. A time-resolved triple probe was found to be an appropriate tool to study the MPP discharge. Different pulse recipes and various discharge parameters can affect the pulsed magnetron plasma, which could be useful for finer and more flexible PVD process control.

ACKNOWLEDGMENTS

The authors would like to gratefully acknowledge Roman Chistyakov and Bassam Abraham (Zond, Inc./Zpulser, LLC) for providing the MPP plasma generator and technical guidance. This study was supported by the Center for Lasers and Plasma in Advanced Manufacturing (National Science Foundation, Grant No. CMMI09-53057).

[1]G. Bräuer, J. Szczyrbowski, and G. Teschner, Surf. Coat. Technol. **94–95**, 658 (1997).
[2]K. Suzuki, Thin Solid Films **351**, 8 (1999).
[3]J. O'Brien and P. J. Kelly, Surf. Coat. Technol. **142–144**, 621 (2001).
[4]I. Swindells, P. J. Kelly, and J. W. Bradley, New J. Phys. **8**, 47 (2006).
[5]A. Mishra, G. Clarke, P. Kelly, and J. W. Bradley, Plasma Processes Polym. **6**, S610 (2009).
[6]K. Sarakinos, J. Alami, and S. Konstantinidis, Surf. Coat. Technol. **204**, 1661 (2010).
[7]V. Kouznetsov, K. Macak, J. M. Schneider, U. Helmersson, and I. Petrov, Surf. Coat. Technol. **122**, 290 (1999).
[8]J. Bohlmark, M. Lattemann, J. T. Gudmundsson, A. P. Ehiasarian, Y. Aranda Gonzalvo, N. Brenning, and U. Helmersson, Thin Solid Films **515**, 1522 (2006).
[9]K. M. Green, D. B. Hayden, D. R. Juliano, and D. N. Ruzic, Rev. Sci. Instrum. **68**, 4555 (1997).
[10]S. Konstantinidis, A. Hemberg, J. P. Dauchot, and M. Hecq, J. Vac. Sci. Technol. B **25**, L19 (2007).
[11]A. P. Ehiasarian, J. G. Wen, and I. Petrov, J. Appl. Phys. **101**, 054301 (2007).
[12]J. A. Davis, W. D. Sproul, D. J. Christie, and M. Geisler, 47th Annual Technical Conference Proceedings of the Society of Vacuum Coaters, Dallas, TX, 2004 (unpublished), p. 215.
[13]K. Sarakinos, J. Alami, and M. Wuttig, J. Phys. D: Appl. Phys. **40**, 2108 (2007).
[14]R. Chistyakov and B. Abraham, 51st Annual Technical Conference Proceedings of the Society of Vacuum Coaters, Chicago, IL, 2008 (unpublished), p. 63.
[15]J. Lin, J. J. Moore, W. D. Sproul, B. Mishra, J. A. Rees, Z. Wu, R. Chistyakov, and B. Abraham, Surf. Coat. Technol. **203**, 3676 (2009).
[16]J. Lin, J. J. Moore, W. D. Sproul, B. Mishra, Z. Wu, and J. Wang, Surf. Coat. Technol. **204**, 2230 (2010).
[17]A. P. Ehiasarian, R. New, W.-D. Münz, L. Hultman, U. Helmersson, and V. Kouznetsov, Vacuum **65**, 147 (2002).
[18]T. Welzel, T. Dunger, H. Kupfer, and F. Richter, J. Appl. Phys. **96**, 6994 (2004).
[19]J. W. Bradley, H. Bäcker, P. J. Kelly, and R. D. Arnell, Surf. Coat. Technol. **135**, 221 (2001).
[20]J. Alami, J. T. Gudmundsson, J. Bohlmark, J. Birch, and U. Helmersson, Plasma Sources Sci. Technol. **14**, 525 (2005).
[21]P. M. Bryant, S. A. Voronin, J. W. Bradley, and A. Vetushka, J. Appl. Phys. **102**, 043302 (2007).
[22]S. Chen and T. Sekiguchi, J. Appl. Phys. **36**, 2363 (1965).
[23]C. Riccardi, G. Longoni, G. Chiodini, and M. Fontanesi, Rev. Sci. Instrum. **72**, 461 (2001).
[24]A. Belkind, A. Freilich, and R. Scholl, J. Vac. Sci. Technol. A **17**, 1934 (1999).
[25]J. E. Sansonetti, W. C. Martin, and S. L. Young, Handbook of Basic Atomic Spectroscopic Data (version 1.1), NIST Physical Data, http://physics.nist.gov/PhysRefData/Handbook (2004).
[26]J. Alami, K. Sarakinos, G. Mark, and M. Wuttig, Appl. Phys. Lett. **89**, 154104 (2006).
[27]S. Konstantinidis, J. P. Dauchot, M. Ganciu, A. Ricard, and M. Hecq, J. Appl. Phys. **99**, 013307 (2006).
[28]D. R. Juliano, D. N. Ruzic, M. M. C. Allain, and D. B. Hayden, J. Appl. Phys. **91**, 605 (2002).
[29]S. M. Rossnagel and H. R. Kaufman, J. Vac. Sci. Technol. A **5**, 2276 (1987).